Electronic Supplementary Material (ESI) for Catalysis Science & Technology.
This journal is © The Royal Society of Chemistry 2022

Supplementary information

Multi-stepwise electron transfer *via* MOF-based nanocomposites for photocatalytic ammonia synthesis

Hanjie Ren [a,b‡], Jiangdan Tan [a,b‡], Zhanfeng Zhao [a,b], Yonghui Shi [a,b], Xin Xin [a,b], Dong Yang [c,d,**],Zhongyi Jiang [a,b,e,*]

[a] Key Laboratory for Green Chemical Technology of Ministry of Education, School of Chemical Engineering and Technology, Tianjin University, Tianjin 300072, People's Republic of China

[b] Collaborative Innovation Center of Chemical Science and Engineering (Tianjin), Tianjin 300072, People's Republic of China

[c] Key Laboratory of Systems Bioengineering of Ministry of Education, School of Chemical Engineering and Technology, Tianjin University, Tianjin 300072, China

[d] School of Environmental Science and Engineering, Tianjin University, Tianjin 300072, China

[e] Joint School of National University of Singapore and Tianjin University, International Campus of Tianjin University, Binhai New City, Fuzhou, 350207, P. R. China

[*] Corresponding authors at: Key Laboratory for Green Chemical Technology of Ministry of Education, School of Chemical Engineering and Technology, Tianjin University, Tianjin 300072, China.

[**] Corresponding author at: Key Laboratory of Systems Bioengineering of Ministry of Education, School of Chemical Engineering and Technology, Tianjin University, Tianjin, 300072, China.

E-mail addresses: dongyang@tju.edu.cn (D. Yang), zhyjiang@tju.edu.cn. (Z. Jiang).

[‡] Hanjie Ren and Jiangdan Tan contributed equally to the work.

CONTENT

1. Supporting Experimental Section

1.1. Chemicals

Zirconium tetrachloride ($ZrCl_4$, ≥ 99.5%), ferric chloride anhydrous ($FeCl_3$, ≥ 99%) and titanium dioxide (TiO_2, P25) were purchased from Macklin Biochemical Reagent Co., Ltd. (Shanghai, China). Melamine ($C_3H_6N_6$, AR), terephthalic acid (TPA, ≥ 98%) and tris (hydroxymethyl) aminomethane (Tris, AR) were supplied from Heowns Biochemical Technology Co., Ltd. Dopamine hydrochloride (≥ 98%), N, N-dimethylformamide (DMF, ≥ 99.9%), methanol (CH_3OH, ≥ 99.5%), ethanol (C_2H_5OH, AR) and acetic acid (HAc, ≥ 99.7%) were received from Aladdin Chemistry Co. Ltd (Shanghai, China). Sodium sulfide (Na_2S, AR) was provided by Damao Chemical Reagent Factory (Tianjin, China). Cadmium sulfate ($CdSO_4$, ≥ 99 %) was supplied by Bailingwei Technology Co. Ltd. (Beijing, China). Hydrochloric acid (HCl, AR) was purchased from Guangfu Corporation (Tianjin, China). Potassium sulfite (K_2SO_3, ≥ 98%) was bought from Energy Chemical (Shanghai, China). All chemicals were used without further purification.

1.2. Ion chromatography method

Typically, 10 mg photocatalysts, 79 mg hole scavengers (K_2SO_3) and 100 mL ultrapure water were added to the reactor. Before light illumination, the mixed solution bubbled with N_2 with the rate of 60 mL min^{-1} and stirred at 500 rpm for 30 min in the dark. Then, the reactor was irradiated by a xenon lamp (300 W, Beijing Merry Change Technology Co., Ltd, MC-PF300B). 1 mL reaction solution was taken every 30 min and filtrated by 13 mm 0.22 μm membrane luer syringe filter twice. The filtrated solution was injected and tested by the ion chromatography (IC, Thermo ICS-600, US). The eluent is 20 mmol L^{-1} methanesulfonic acid, eluent flow rate is 1.0 mL min^{-1}, the temperature is ambient temperature, the detection is suppressed conductivity, the suppressor is Dionex cation self-regenerating suppressor and AutoSuppression recycle mode, the applied current is 59 mA, injection volume is 10 μL, and the storage solution is eluent.

1.3. $^{15}N_2$ isotope labeling experiments

The $^{15}N_2$ isotope labeling experiments were measured *via* the nuclear magnetic resonance (NMR) method (500 MHz, Varian Inova, USA). First, 5 mL reaction liquid was filtrated by 13 mm 0.22 μm membrane luer syringe filter twice to remove solid catalysts. Afterward, the obtained solution was adjusted by 6 mol L^{-1} H_2SO_4 solution to pH = 1.3. Finally, 100 mL DMSO-d_6 was added to 1 mL acidized solution and mixed adequately.

1.4. Electrochemical measurements

The photocurrent response and electrochemical impedance spectra (EIS) of photocatalysts were conducted by the electrochemical experiments on a CHI660D electrochemical workstation. A three-electrode system consisting of a reference electrode (Ag/AgCl), a counter electrode (Pt foil) and a working electrode was constructed, and Na_2SO_4 solution (0.1 mol L^{-1}) was employed as the electrolyte. The preparation process of working electrode was as below: 10 mg photocatalyst was dispersed in 1 mL of aqueous Nafion solution (10 vol%), and then the suspension was ultrasonically operated for 20 min. Thereafter, the suspension was dripped on the surface of a 1 × 2 cm^2 fluorine-doped tin oxide (FTO) glass, which was subsequently placed in a 40 °C oven all night. In the EIS Nyquist plot and transient photocurrent, initial voltage, alternating voltage and frequency were -0.1 V, 5 mV and 10^5-10^{-2} Hz, respectively. A 300 W xenon lamp was applied as the illuminant. The conduction band potential (E_{cb}) (*vs.* Ag/AgCl) is approximately equal to flat band potential (E_{fb}) (*vs.* Ag/AgCl) minus 0.1 eV, and E_{cb} (*vs.* NHE) is approximately equal to E_{cb} (*vs.* Ag/AgCl) plus 0.2 eV.

1.5. Determination of apparent quantum efficiency (AQE) and solar-to-ammonia (STA) efficiency

For measurement of the N_2-reduction apparent quantum efficiency (AQE), the photocatalytic NH_3 evolution was carried out under monochromatic light using bandpass filters (center wavelengths: 380, 405, 420, 450 and 500 nm, full width at half

maximum for all: 20 nm, Beijing China Education Au-light Co., Ltd.). The corresponding power density was measured using an optical power meter (CEL-NP2000).

The AQE was calculated according to the following equation:

$$\mathrm{AQE} = \frac{\mathrm{N_{reacted}}}{\mathrm{N_{incident}}} = \frac{3 \times \mathrm{N_{(NH_3)}}}{\frac{\mathrm{Pt}}{\mathrm{h\upsilon}}} = \frac{3 \times \mathrm{n_{(NH_3)}} \times \mathrm{N_A}}{\frac{\mathrm{Pt\lambda}}{\mathrm{hc}}} \times 100\%$$

where $N_{(NH3)}$ is the number of the generated ammonia molecules, $n_{(NH3)}$ is the mole of the generated ammonia molecules, N_A is Avogadro constant, P is the xenon lamp power, t is the irradiation time, h is Planck constant, v is the light frequency and c is the speed of light in free space.

The solar-to-ammonia (STA) efficiency was calculated according to the following equation:

$$\text{STA efficiency} = \frac{\Delta \mathrm{G_{(NH_3)}} \times \mathrm{n_{(NH_3)}}}{\mathrm{Pt}} \times 100\%$$

where $\Delta G_{(NH3)}$ value is the Gibbs free energy for NH_3 generation from water and N_2 (339 kJ mol^{-1}), $n_{(NH3)}$ is the mole of the generated ammonia molecules, P is xenon lamp power and t is the irradiation time.

To determine the AQE and STA efficiency, the reactions were carried out in a photocatalytic reactor under xenon light irradiation. Typically, 10 mg photocatalysts, 79 mg hole scavengers (K_2SO_3) and 100 mL ultrapure water were added to the reactor. Before light illumination, the mixed solution bubbled with N_2 and stirred at 500 rpm for 30 min in the dark. Then, the reactor was irradiated by a xenon lamp. At regular intervals, 1 mL filtrated solution was tested by ion chromatography (IC).

1.6. Photocatalytic H_2 evolution

In typical experiment, 10 mg photocatalysts and 10 mL triethanolamine (TEOA) as hole scavenger were poured into 100 mL deionized water in turn. Under the illumination of xenon lamp for 1 h, 3 wt% Pt as co-catalyst was photodeposited on the sample in quartz reactor. The system was evacuated to remove the gas dissolved in the solution and keep pressure balanced around the system cycling by a vacuum pump.

Photocatalytic H_2 evolution rates of all prepared samples were determined by Techcomp GC7900 gas chromatography (equipped with TCD) under full spectrum. Every 30 min, the generated gas was fetched from the photocatalytic reactor and injected in gas chromatography to analyze the H_2 yield.

2. Characterization Methods

The morphology and microstructure of photocatalysts were reflected by scanning electron microscopy (SEM, Regulus 8100, Japan) and transmission electron microscopy (TEM, JEOL JEM-F200, Japan). The characteristic peaks of crystal structure were recorded through X-ray powder diffraction (XRD, Smartlab, Japan) patterns using Rigaku D/max 2500 V/PC X-ray diffractometer (Cu Kα, λ = 0.154 nm). The data were collected from 5 ° to 60 ° with a step increment of 2θ = 0.02 ° at a rate of 10 ° min^{-1} for wide-angle X-ray (WAXS). Fourier transform infrared spectroscopy (FTIR) of photocatalysts was performed by adopting a Nicolet-560 Fourier transform infrared spectrometer. The composition and chemical status of photocatalysts were characterized by employing the X-ray photoelectron spectroscopy (XPS, K-Alpha+) on a PerkinElmer PHI 1600 ESCA X-ray spectrometer using C 1s at 284.6 eV as an internal standard calibration peak. Photoluminescence (PL, UK) fluorescence spectra and transient fluorescence lifetimes were conducted by an Edinburgh Instruments FLS1000 fluorescence spectrometer with an excitation wavelength of 320 nm. The UV-vis diffuse reflection spectra (DRS) of photocatalysts were acquired by a Hitachi U-3010 UV-vis spectrophotometer. The reaction solution was measured by IC (Thermo ICS-600, US) to determine the ammonia concentration. The $^{15}N_2$ isotope labeling experiments were measured by NMR (500 MHz, Varian Inova, USA) to confirm that the detectable NH_3 is indeed generated from N_2 gas.

3. Theoretical Calculations

Density functional theory (DFT) simulations were performed to calculate the N_2 activation with Cambridge Sequential Total Energy Package (CASTEP) software in Materials Studio 2019 [1-4]. The calculated lattice parameters for primary unit cell of UiO-66 with 12 Zr, 96 C, 64 O and 72 H atoms is a = 14.5 Å, b = 14.5 Å, c = 20.6 Å, and α = 90.0 º, β = 90.0 º, γ = 90.0 º; while that of CNNS with 24 C and 32 N atoms is a = 12.8 Å, b = 14.8 Å, c = 5.0 Å, and α = 90.0 º, β = 90.0 º, γ = 90.0 º; and that of PDA with 32 C, 4 N, 8 O and 22 H atoms is a = 14.5 Å, b = 16.1 Å, c = 5.0 Å, and α = 90.0 º, β = 90.0 º, γ = 90.0 º. The calculated lattice parameters for primary unit cell of UPC with 12 Zr, 152 C, 36 N, 72 O and 104 H atoms is a = 14.0 Å, b = 15.1 Å, c = 29.4 Å, and α = 90.0 º, β = 90.0 º, γ = 90.0 º; while that of UiO-66 /CNNS with 12 Zr, 120 C, 32 N, 64 O and 82 H atoms is a = 13.7 Å, b = 14.7 Å, c = 27.0 Å, and α = 90.0 º, β = 90.0 º, γ = 90.0 º, which are consisted of the unit cells of UiO-66, CNNS and PDA. All the molecular structures were consistent with the actual situation of the experiments and literature (**Figure S1** and **2**, and **Table S1-4**) [5-10]. All structures were optimized by the Forcite module with Universal Force Field (UFF) and the CASTEP software package for the first principles was exploited for DFT calculation in this work. As for the Forcite module, the energy convergence tolerance was 10^{-4} kcal mol^{-1}, the force convergence tolerance was 5×10^{-3} kcal mol^{-1} $Å^{-1}$, the stress convergence tolerance was 5×10^{-3} GPa, and the displacement convergence tolerance was 5×10^{-5} Å, respectively. As for the CASTEP software package, the electron exchange and correlation were described by Perdew-Burke-Ernzerhof (PBE) functional within Generalized-gradient approximation (GGA) [11, 12]. The cut-off energy was fitted to 489 eV with plane-wave basis. The Brillouin zone was sampled with 1 × 1 × 1 k-point for structural optimization and calculations. Geometry optimization was accomplished before energy calculation. A supercell with two layers was used as a support to model the UPC (1 1 1) and UiO-66 (1 1 1) surface, while the top layer was allowed to relax and the bottom

layer was constrained. The vacuum region was set as 10 Å to prevent the interaction between two neighboring layers.

The grand canonical Monte Carlo (GCMC) for Sorption module was used to simulate the adsorption process and distribution plots of N_2 molecules in the UPC and UiO-66 models with UFF [13]. The N_2 adsorption of models was simulated at 298 K and 101.3 kPa. The method was set to metropolis, while the equilibration steps and production steps were adjusted to 10^7.

In the calculations, because of the complexity of calculations and the relative limitations of CASTEP in the calculations, the models do not describe the interactions and structural changes between units, while they are not optimized over spin states and transition state barriers were not included. Thus, the models were only intended to give mostly qualitative insights.

4. Supporting Data

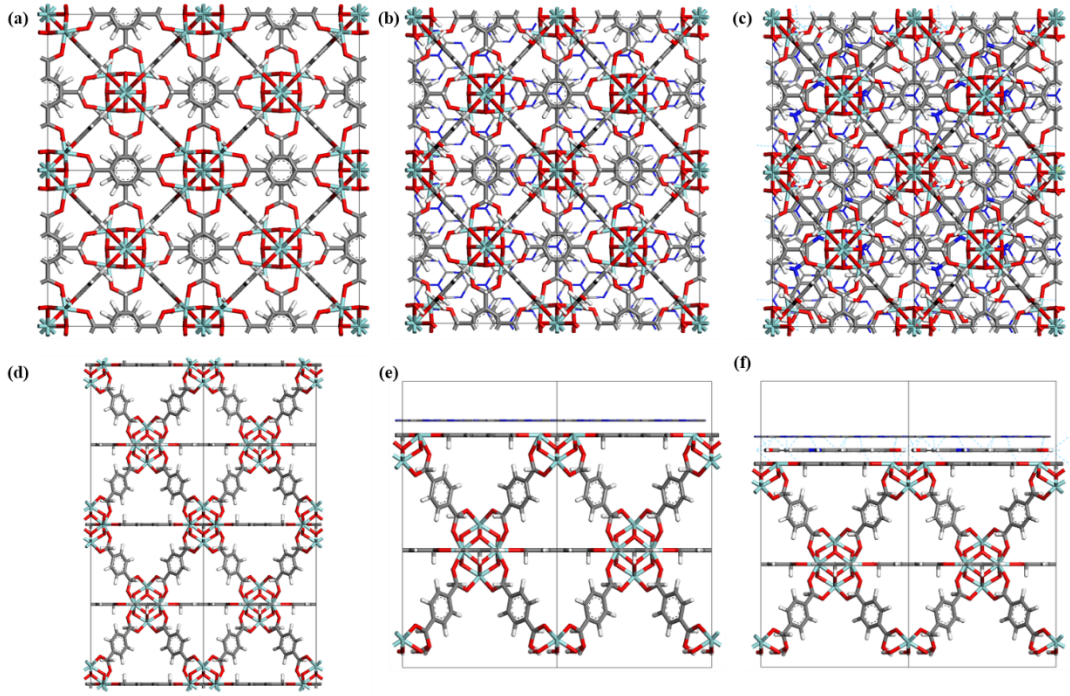

Fig. S1 Schematic diagrams of (a, d) UiO-66, (b, e) UC and (c, f) UPC unit cells. Key: green balls, Zr; grey balls, C; blue balls, N; red balls: O; white ball, H, light blue dotted line: hydrogen bond.

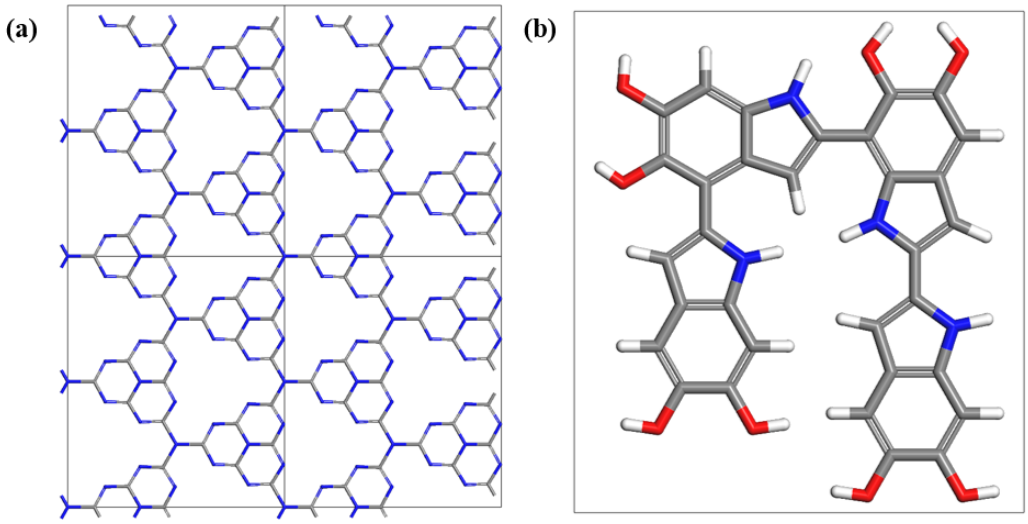

Fig. S2 Schematic diagrams of (a) CNNS and (b) PDA unit cells. Key: grey balls, C; blue balls, N; red balls: O; white ball, H.

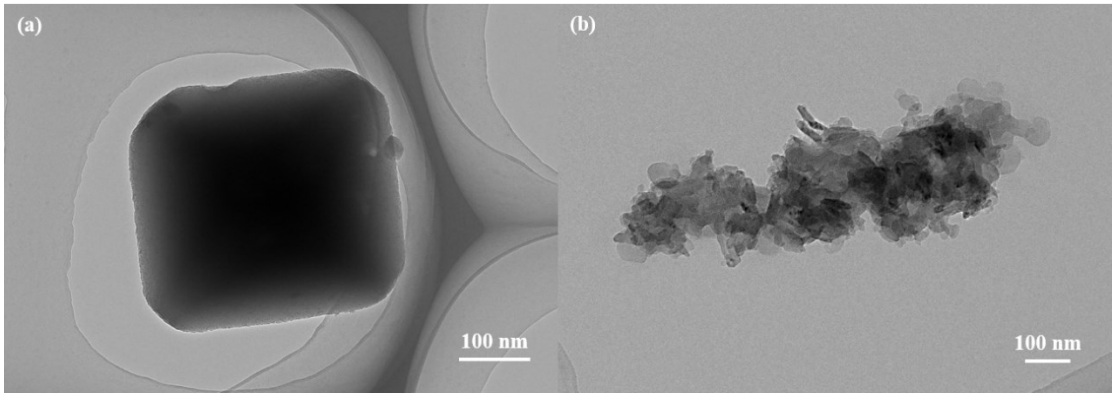

Fig. S3 TEM images of (a) UiO-66/PDA and (b) CNNS samples.

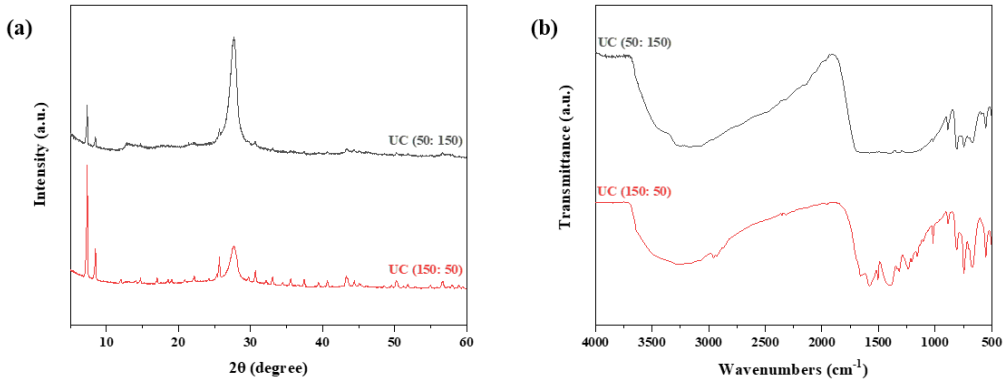

Fig. S4 (a) XRD patterns and (b) FTIR spectra of UC (50: 150) and UC (150: 50) samples.

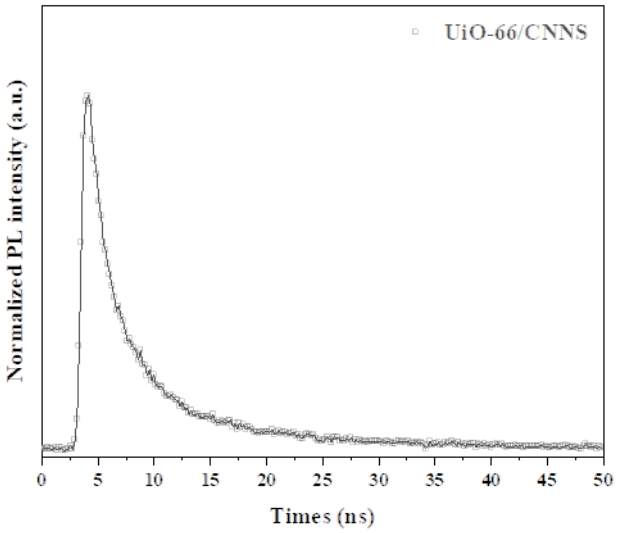

Fig. S5 The transient fluorescence lifetime decay curve of UC.

The average fluorescent lifetimes are obtained by the transient fluorescence lifetime decay curves and the following equation:

$$\tau_{AvInt} = \frac{B_1\tau_1^2 + B_2\tau_2^2 + B_3\tau_3^2}{B_1\tau_1 + B_2\tau_2 + B_3\tau_3}$$

where τ_1, τ_2 and τ_3 are the fluorescent lifetimes, B_1, B_2 and B_3 are the corresponding amplitudes.

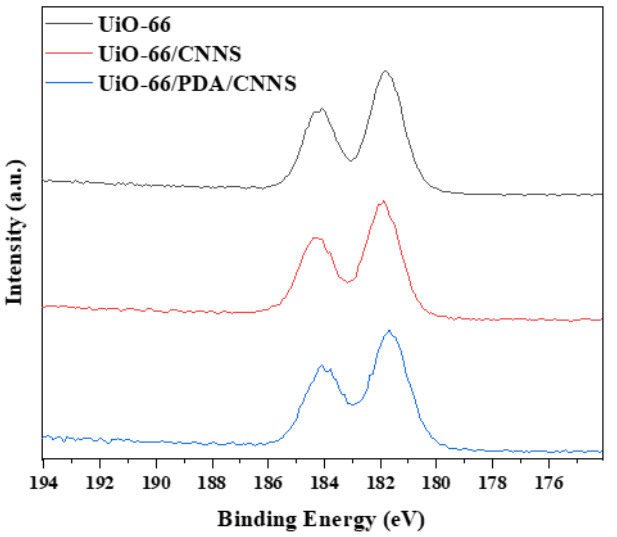

Fig. S6 High-resolution Zr 3d XPS spectra of UiO-66, UC and UPC.

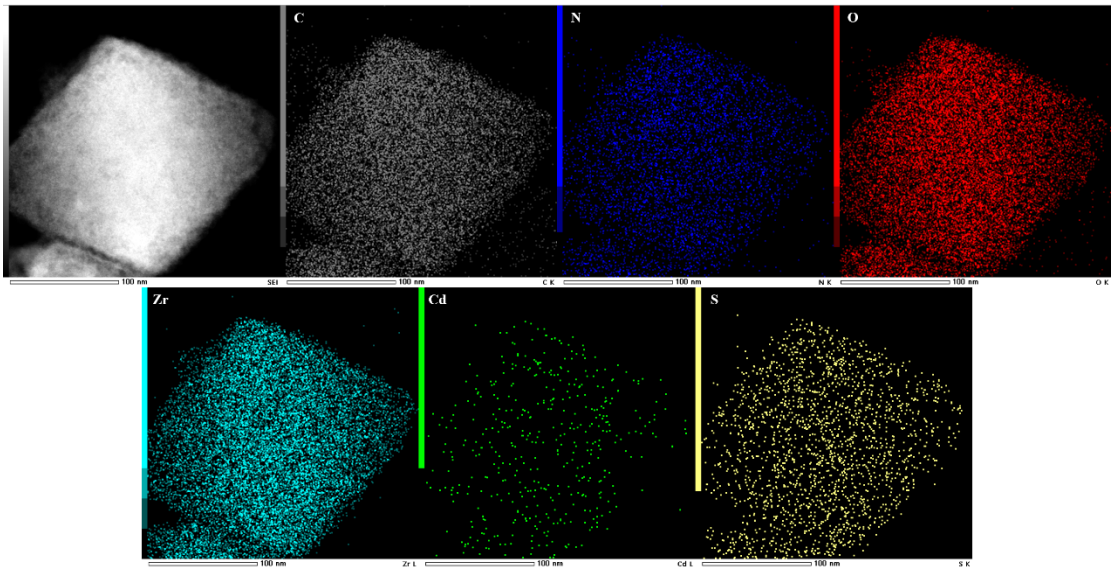

Fig. S7 The STEM image and corresponding element mappings of C, N, O, Zr, Cd and S of UPCdS.

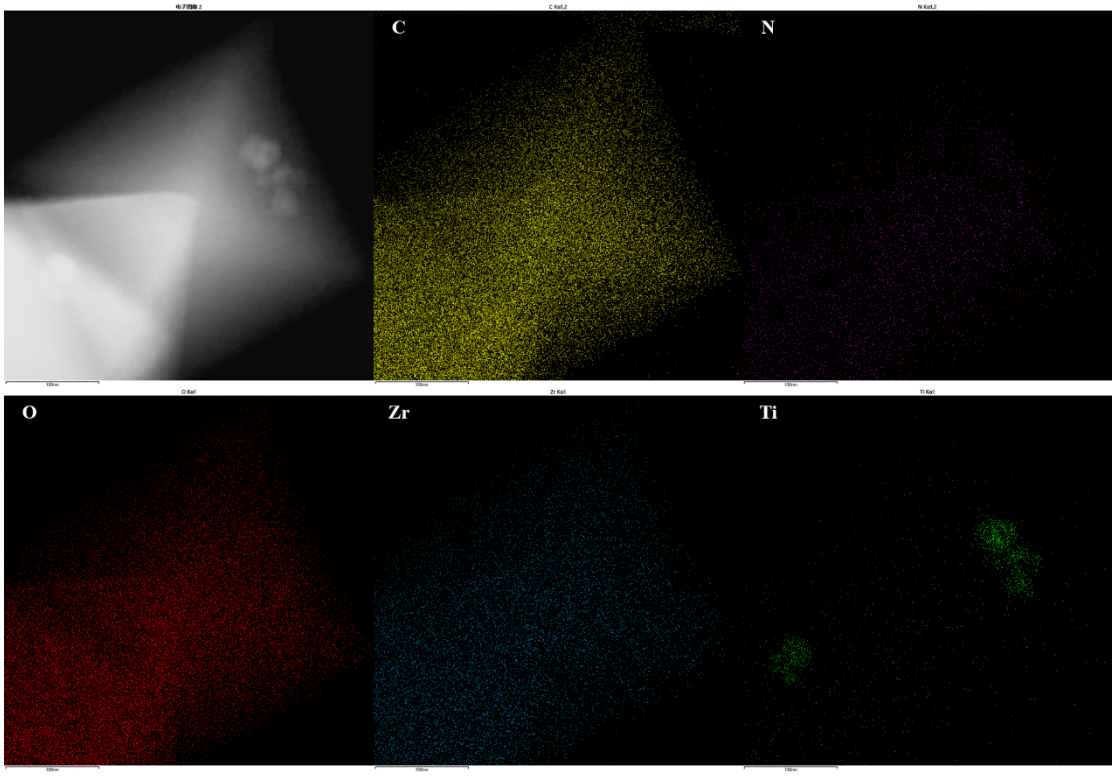

Fig. S8 The STEM image and corresponding element mappings of C, N, O, Zr and Ti of UPT.

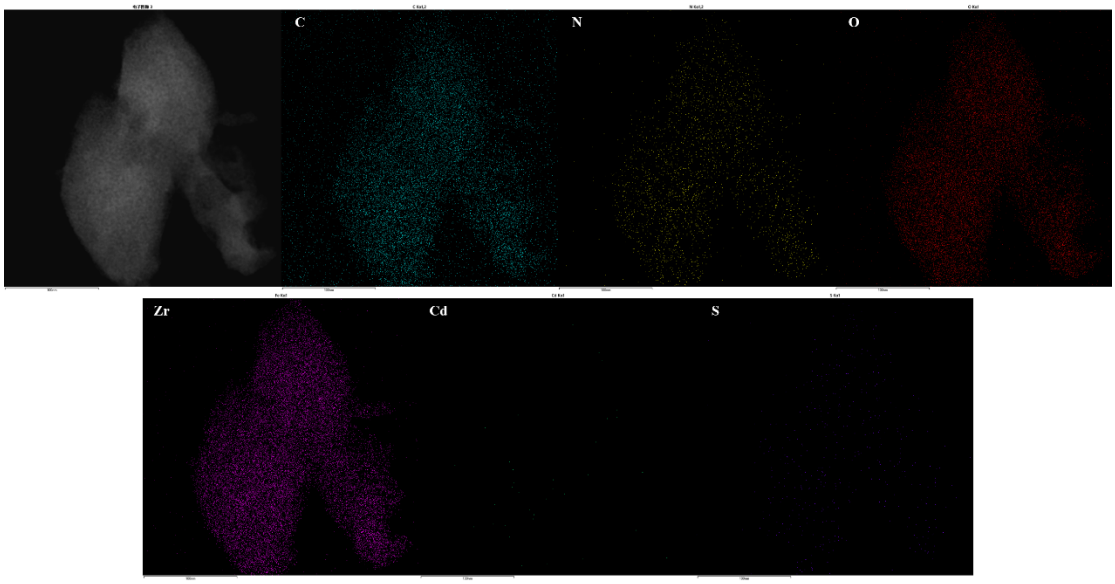

Fig. S9 The STEM image and corresponding element mappings of C, N, O, Zr, Cd and S of MPCdS.

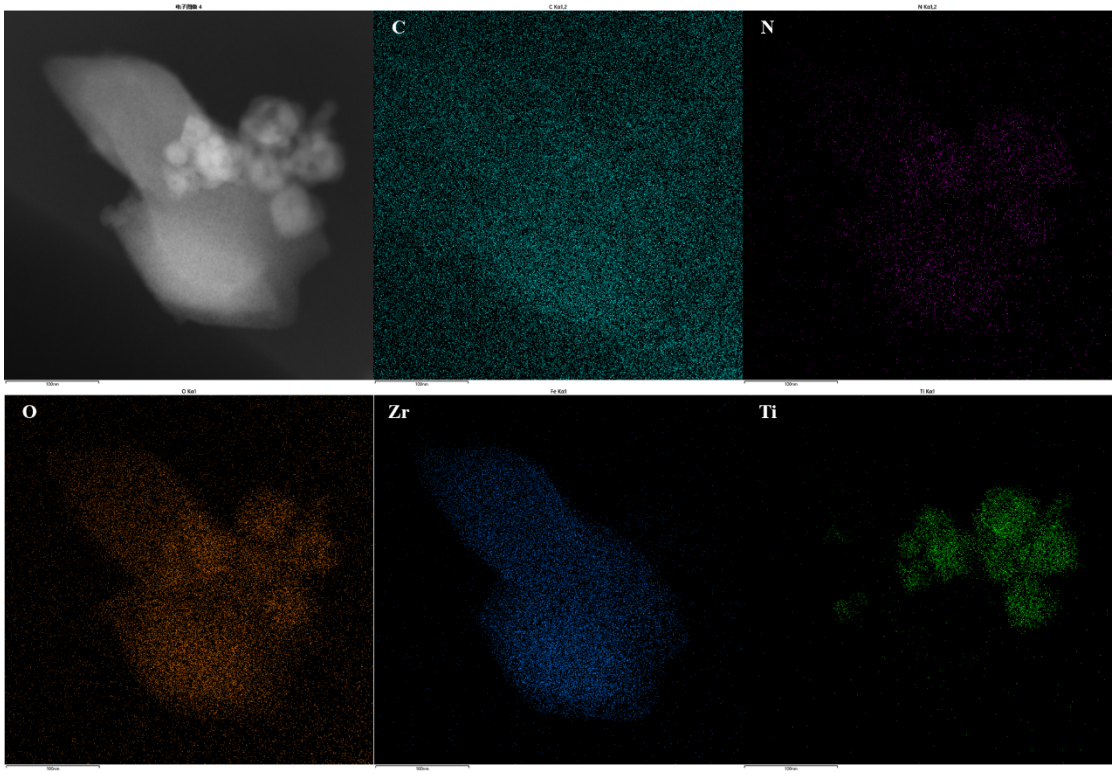

Fig. S10 The STEM image and corresponding element mappings of C, N, O, Zr and Ti of MPT.

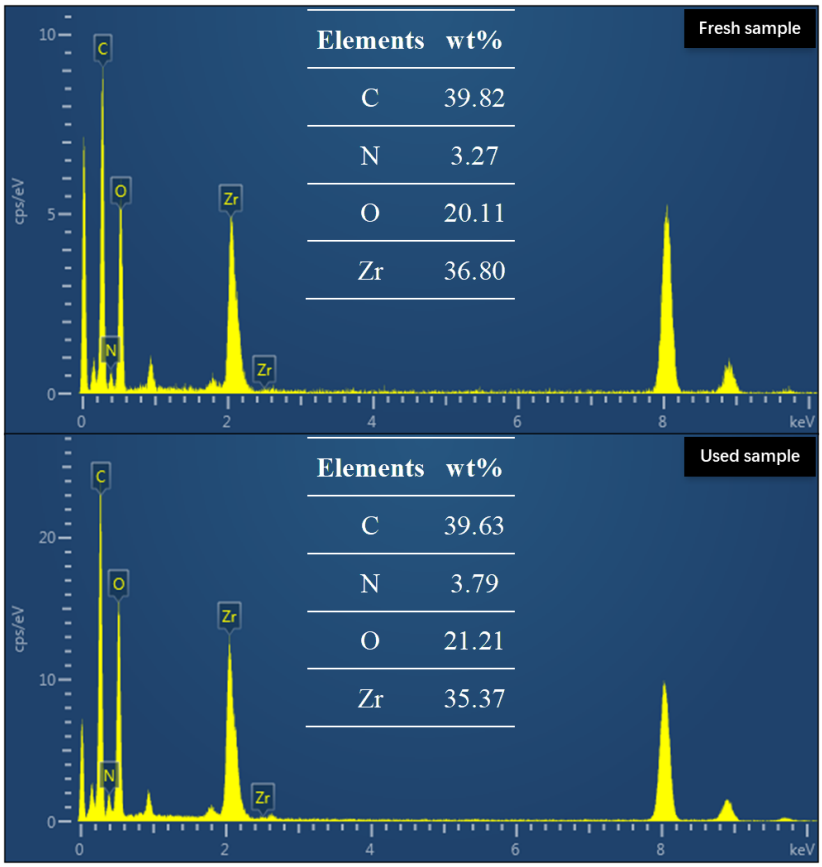

Fig. S11 EDS spectra of UPC before and after photocatalytic reaction.

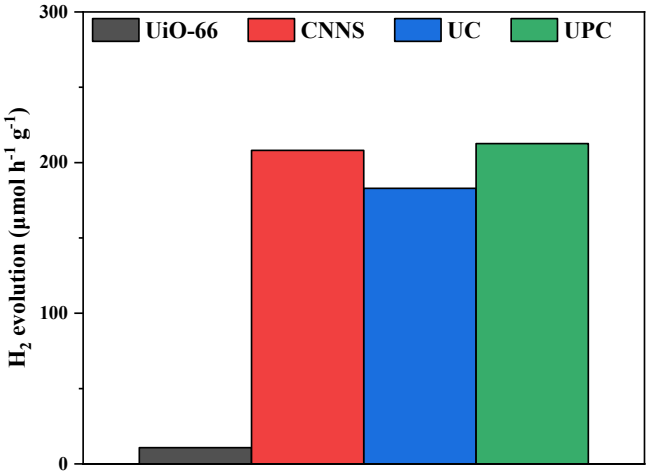

Fig. S12 H_2 evolution rates of UiO-66, CNNS, UC and UPC samples under full spectrum.

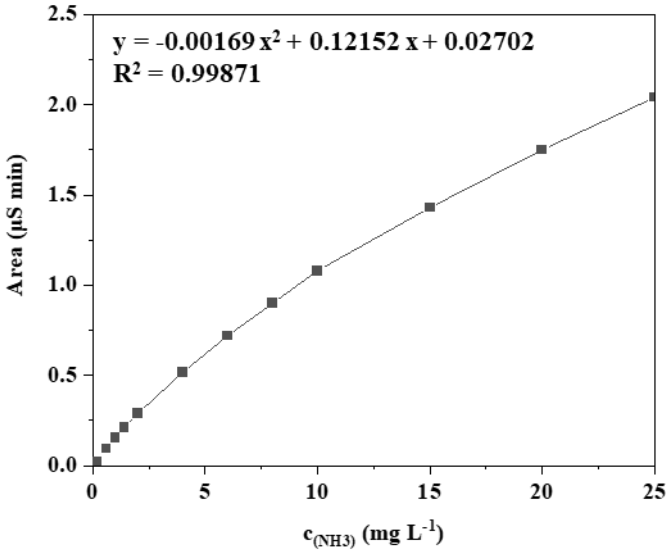

Fig. S13 The standard curve for NH_3 using the ion chromatography method.

5. Tables

Table S1 The lattice parameters and cell angles of UiO-66, CNNS and PDA unit cells.

UiO-66				**CNNS**				**PDA**			
Lattice parameters (Å)		**Cell angles (°)**		**Lattice parameters (Å)**		**Cell angles (°)**		**Lattice parameters (Å)**		**Cell angles (°)**	
a	14.5	α	90.0	a	12.8	α	90.0	a	14.5	α	90.0
b	14.5	β	90.0	b	14.8	β	90.0	b	16.1	β	90.0
c	20.6	γ	90.0	c	5.0	γ	90.0	c	5.0	γ	90.0

Table S2 The lattice parameters and cell angles of UPC and UC unit cells.

UPC				**UC**			
Lattice parameters (Å)		**Cell angles (°)**		**Lattice parameters (Å)**		**Cell angles (°)**	
a	14.0	α	90.0	a	13.7	α	90.0
b	15.1	β	90.0	b	14.7	β	90.0

c	29.4	γ	90.0	c	27.0	γ	90.0

Table S3 The coordinates of different atoms of UiO-66, CNNS and PDA models.

Element	Fractional coordinates UiO-66			Element	Fractional coordinates CNNS			Element	Fractional coordinates PDA		
	u	v	w		u	v	w		u	v	w
C	10.7	10.7	16.8	C	1.6	0.0	0	C	9.5	-4.0	0
C	3.4	3.4	6.5	C	1.6	7.4	0	C	10.2	-5.3	0
C	3.9	3.9	16.8	C	8.0	3.7	0	C	11.8	-5.3	0
C	11.2	11.2	6.5	C	8.0	11.1	0	C	12.6	-4.0	0
C	11.2	11.2	14.1	C	5.6	5.1	0	C	11.8	-2.7	0
C	3.9	3.9	3.8	C	5.6	12.4	0	C	10.2	-2.7	0
C	3.4	3.4	14.1	C	12.0	1.4	0	C	12.3	-6.8	0
C	10.7	10.7	3.8	C	12.0	8.7	0	C	11.0	-7.7	0
C	8.0	1.2	20.6	C	5.6	2.3	0	C	5.6	-3.2	0
C	0.7	8.5	10.3	C	5.6	9.7	0	C	5.6	-4.8	0
C	1.2	8.0	20.6	C	12.0	6.0	0	C	7.0	-5.2	0
C	8.5	0.7	10.3	C	12.0	13.4	0	C	7.9	-4.0	0
C	6.6	13.3	20.6	C	3.6	6.2	0	C	4.2	-2.5	0
C	13.8	6.1	10.3	C	3.6	13.5	0	C	2.9	-3.2	0
C	13.3	6.6	20.6	C	10.0	2.5	0	C	2.9	-4.8	0
C	6.1	13.8	10.3	C	10.0	9.9	0	C	4.2	-5.5	0
C	11.9	2.7	15.1	C	5.7	0.0	0	C	3.0	-8.0	0
C	4.6	10.0	4.8	C	5.7	7.4	0	C	3.5	-9.4	0
C	4.6	10.0	15.8	C	12.1	3.7	0	C	5.0	-9.4	0
C	11.9	2.7	5.5	C	12.1	11.1	0	C	4.2	-7.1	0
C	10.0	4.6	15.8	C	3.6	1.2	0	C	5.8	-10.8	0
C	2.7	11.9	5.5	C	3.6	8.6	0	C	5.0	-12.1	0
C	2.7	11.9	15.1	C	10.0	4.9	0	C	3.5	-12.1	0
C	10.0	4.6	4.8	C	10.0	12.3	0	C	2.7	-10.8	0
C	3.4	11.2	14.1	N	2.2	6.2	0	C	9.8	-10.1	0
C	10.7	3.9	3.8	N	2.2	13.6	0	C	10.2	-11.6	0
C	11.2	3.4	14.1	N	8.6	2.5	0	C	11.8	-11.6	0
C	3.9	10.7	3.8	N	8.6	9.9	0	C	11.0	-9.2	0
C	3.9	10.7	16.8	N	6.3	6.2	0	C	12.6	-12.9	0
C	11.2	3.4	6.5	N	6.3	13.6	0	C	11.8	-14.3	0
C	10.7	3.9	16.8	N	12.7	2.5	0	C	10.2	-14.3	0
C	3.4	11.2	6.5	N	12.7	9.9	0	C	9.5	-12.9	0

C	8.0	13.3	20.6	N	4.3	2.4	0	H	13.7	-4.0	0
C	0.7	6.1	10.3	N	4.3	9.8	0	H	13.3	-7.3	0
C	1.2	6.6	20.6	N	10.7	6.1	0	H	8.8	-7.2	0
C	8.5	13.8	10.3	N	10.7	13.5	0	H	7.3	-6.4	0
C	6.6	1.2	20.6	N	6.3	1.2	0	H	7.5	-1.7	0
C	13.8	8.5	10.3	N	6.3	8.6	0	H	4.2	-1.3	0
C	13.3	8.0	20.6	N	12.7	4.9	0	H	1.9	-7.7	0
C	6.1	0.7	10.3	N	12.7	12.3	0	H	6.6	-7.8	0
C	4.6	4.6	15.8	N	4.3	5.0	0	H	6.9	-10.8	0
C	11.9	11.9	5.5	N	4.3	12.4	0	H	1.6	-10.8	0
C	11.9	11.9	15.1	N	10.7	1.3	0	H	8.7	-9.9	0
C	4.6	4.6	4.8	N	10.7	8.7	0	H	13.4	-9.9	0
C	2.7	2.7	15.1	N	2.2	1.2	0	H	13.7	-12.9	0
C	10.0	10.0	4.8	N	2.2	8.6	0	H	8.3	-12.9	0
C	10.0	10.0	15.8	N	8.6	4.9	0	H	10.1	-0.5	0
C	2.7	2.7	5.5	N	8.6	12.3	0	H	11.9	-0.5	0
C	12.4	12.4	17.5	N	0.0	0.0	0	H	0.9	-5.0	0
C	5.1	5.1	7.2	N	0.0	7.4	0	H	1.6	-1.6	0
C	11.6	11.6	16.4	N	6.4	3.7	0	H	8.5	-15.5	0
C	4.3	4.3	6.1	N	6.4	11.1	0	H	13.6	-15.5	0
C	2.2	2.2	17.5	N	4.3	0.0	0	H	1.7	-13.3	0
C	9.4	9.4	7.2	N	4.3	7.4	0	H	6.8	-13.3	0
C	2.9	2.9	16.4	N	10.7	3.7	0	N	9.8	-6.8	0
C	10.2	10.2	6.1	N	10.7	11.1	0	N	7.0	-2.8	0
C	9.4	9.4	13.3					N	5.5	-8.0	0
C	2.2	2.2	3.1					N	12.3	-10.1	0
C	10.2	10.2	14.4					O	9.5	-1.3	0
C	2.9	2.9	4.1					O	12.6	-1.3	0
C	5.1	5.1	13.3					O	1.6	-5.5	0
C	12.4	12.4	3.1					O	1.6	-2.5	0
C	4.3	4.3	14.4					O	9.5	-15.6	0
C	11.6	11.6	4.1					O	12.6	-15.6	0
C	10.2	14.5	20.6					O	2.7	-13.4	0
C	2.9	7.3	10.3					O	5.8	-13.4	0
C	8.7	14.5	20.6								
C	1.4	7.3	10.3								
C	14.5	10.2	20.6								
C	7.3	2.9	10.3								
C	14.5	8.7	20.6								
C	7.3	1.4	10.3								

C	4.3	0.0	20.6
C	11.6	7.3	10.3
C	5.9	14.5	20.6
C	13.1	7.3	10.3
C	14.5	4.3	20.6
C	7.3	11.6	10.3
C	14.5	5.9	20.6
C	7.3	13.1	10.3
C	12.4	2.2	17.5
C	5.1	9.4	7.2
C	11.6	2.9	16.4
C	4.3	10.2	6.1
C	5.1	9.4	13.3
C	12.4	2.2	3.1
C	4.3	10.2	14.4
C	11.6	2.9	4.1
C	9.4	5.1	13.3
C	2.2	12.4	3.1
C	10.2	4.3	14.4
C	2.9	11.6	4.1
C	2.2	12.4	17.5
C	9.4	5.1	7.2
C	2.9	11.6	16.4
C	10.2	4.3	6.1
H	10.4	10.4	17.9
H	3.2	3.2	7.6
H	4.1	4.1	17.9
H	11.4	11.4	7.6
H	11.4	11.4	13.0
H	4.1	4.1	2.7
H	3.2	3.2	13.0
H	10.4	10.4	2.7
H	8.5	2.2	20.6
H	1.3	9.5	10.3
H	2.2	8.5	20.6
H	9.5	1.3	10.3
H	6.0	12.3	20.6
H	13.3	5.1	10.3
H	12.3	6.0	20.6
H	5.1	13.3	10.3

H	12.6	1.9	14.8
H	5.4	9.2	4.5
H	5.4	9.2	16.1
H	12.6	1.9	5.8
H	9.2	5.4	16.1
H	1.9	12.6	5.8
H	1.9	12.6	14.8
H	9.2	5.4	4.5
H	3.2	11.4	13.0
H	10.4	4.1	2.7
H	11.4	3.2	13.0
H	4.1	10.4	2.7
H	4.1	10.4	17.9
H	11.4	3.2	7.6
H	10.4	4.1	17.9
H	3.2	11.4	7.6
H	8.5	12.3	20.6
H	1.3	5.1	10.3
H	2.2	6.0	20.6
H	9.5	13.3	10.3
H	6.0	2.2	20.6
H	13.3	9.5	10.3
H	12.3	8.5	20.6
H	5.1	1.3	10.3
H	5.4	5.4	16.1
H	12.6	12.6	5.8
H	12.6	12.6	14.8
H	5.4	5.4	4.5
H	1.9	1.9	14.8
H	9.2	9.2	4.5
H	9.2	9.2	16.1
H	1.9	1.9	5.8
H	10.2	8.6	13.3
H	3.0	1.4	3.1
H	4.3	5.9	13.3
H	11.6	13.2	3.1
H	7.3	2.9	9.1
H	0.0	10.2	1.1
H	4.3	14.5	19.4
H	11.6	7.3	9.1

H	1.4	11.6	17.5
H	8.6	4.3	7.2
H	4.3	8.6	13.3
H	13.2	3.0	3.1
H	10.2	5.9	13.3
H	3.0	13.2	3.1
H	13.2	3.0	17.5
H	4.3	8.6	7.2
H	2.9	7.3	9.1
H	10.2	14.5	-1.1
H	14.5	4.3	21.7
H	7.3	11.6	9.1
H	11.6	13.2	17.5
H	4.3	5.9	7.2
H	3.0	1.4	17.5
H	8.6	10.2	7.2
O	12.0	12.0	18.8
O	4.8	4.8	8.6
O	2.5	2.5	18.8
O	9.8	9.8	8.6
O	9.8	9.8	12.0
O	2.5	2.5	1.7
O	4.8	4.8	12.0
O	12.0	12.0	1.7
O	10.8	1.3	20.6
O	3.5	8.6	10.3
O	1.3	10.8	20.6
O	8.6	3.5	10.3
O	3.7	13.2	20.6
O	11.0	6.0	10.3
O	13.2	3.7	20.6
O	6.0	11.0	10.3
O	13.3	1.2	17.0
O	6.1	8.5	6.7
O	6.1	8.5	13.8
O	13.3	1.2	3.6
O	8.5	6.1	13.8
O	1.2	13.3	3.6
O	1.2	13.3	17.0
O	8.5	6.1	6.7

O	4.8	9.8	12.0
O	12.0	2.5	1.7
O	9.8	4.8	12.0
O	2.5	12.0	1.7
O	2.5	12.0	18.8
O	9.8	4.8	8.6
O	12.0	2.5	18.8
O	4.8	9.8	8.6
O	10.8	13.2	20.6
O	3.5	6.0	10.3
O	1.3	3.7	20.6
O	8.6	11.0	10.3
O	3.7	1.3	20.6
O	11.0	8.6	10.3
O	13.2	10.8	20.6
O	6.0	3.5	10.3
O	6.1	6.1	13.8
O	13.3	13.3	3.6
O	13.3	13.3	17.0
O	6.1	6.1	6.7
O	1.2	1.2	17.0
O	8.5	8.5	6.7
O	8.5	8.5	13.8
O	1.2	1.2	3.6
O	12.8	14.5	19.3
O	5.5	7.3	9.0
O	1.8	14.5	19.3
O	9.0	7.3	9.0
O	7.3	9.0	11.5
O	14.5	1.8	1.2
O	7.3	5.5	11.5
O	14.5	12.8	1.2
O	5.5	7.3	11.5
O	12.8	14.5	1.2
O	9.0	7.3	11.5
O	1.8	14.5	1.2
O	14.5	12.8	19.3
O	7.3	5.5	9.0
O	14.5	1.8	19.3
O	7.3	9.0	9.0

Zr	12.9	12.9	20.6
Zr	5.6	5.6	10.3
Zr	1.6	1.6	20.6
Zr	8.9	8.9	10.3
Zr	12.9	1.6	20.6
Zr	5.6	8.9	10.3
Zr	1.6	12.9	20.6
Zr	8.9	5.6	10.3
Zr	14.5	0.0	18.3
Zr	7.3	7.3	8.0
Zr	7.3	7.3	12.6
Zr	14.5	14.5	2.3

Table S4 The coordinates of different atoms of UPS and UC models.

Element	**Fractional coordinates**			**Element**	**Fractional coordinates**		
	UPC				**UC**		
	u	**v**	**w**		**u**	**v**	**w**
C	10.2	11.1	17.1	C	10.0	10.7	17.9
C	3.2	3.5	6.8	C	3.2	3.4	7.1
C	3.7	4.1	17.1	C	3.7	3.9	17.9
C	10.7	11.6	6.8	C	10.5	11.2	7.1
C	10.7	11.6	14.4	C	10.5	11.2	15.1
C	3.7	4.1	4.1	C	3.7	3.9	4.2
C	3.2	3.5	14.4	C	3.2	3.4	15.1
C	10.2	11.1	4.1	C	10.0	10.7	4.2
C	7.6	1.3	20.9	C	7.5	1.2	21.9
C	0.7	8.8	10.6	C	0.7	8.5	11.1
C	1.2	8.3	20.9	C	1.1	8.0	21.9
C	8.1	0.7	10.6	C	8.0	0.7	11.1
C	6.3	13.9	20.9	C	6.2	13.4	21.9
C	13.3	6.3	10.6	C	13.0	6.1	11.1
C	12.8	6.8	20.9	C	12.5	6.6	21.9
C	5.8	14.4	10.6	C	5.7	13.9	11.1
C	11.4	2.8	15.4	C	11.1	2.7	16.1
C	4.4	10.4	5.1	C	4.3	10.0	5.3
C	4.4	10.4	16.1	C	4.3	10.0	16.9
C	11.4	2.8	5.8	C	11.1	2.7	6.0
C	9.6	4.8	16.1	C	9.4	4.6	16.9
C	2.6	12.4	5.8	C	2.5	12.0	6.0
C	2.6	12.4	15.4	C	2.5	12.0	16.1

C	9.6	4.8	5.1	C	9.4	4.6	5.3
C	3.2	11.6	14.4	C	3.2	11.2	15.1
C	10.2	4.1	4.1	C	10.0	3.9	4.2
C	10.7	3.5	14.4	C	10.5	3.4	15.1
C	3.7	11.1	4.1	C	3.7	10.7	4.2
C	3.7	11.1	17.1	C	3.7	10.7	17.9
C	10.7	3.5	6.8	C	10.5	3.4	7.1
C	10.2	4.1	17.1	C	10.0	3.9	17.9
C	3.2	11.6	6.8	C	3.2	11.2	7.1
C	7.6	13.9	20.9	C	7.5	13.4	21.9
C	0.7	6.3	10.6	C	0.7	6.1	11.1
C	1.2	6.8	20.9	C	1.1	6.6	21.9
C	8.1	14.4	10.6	C	8.0	13.9	11.1
C	6.3	1.3	20.9	C	6.2	1.2	21.9
C	13.3	8.8	10.6	C	13.0	8.5	11.1
C	12.8	8.3	20.9	C	12.5	8.0	21.9
C	5.8	0.7	10.6	C	5.7	0.7	11.1
C	4.4	4.8	16.1	C	4.3	4.6	16.9
C	11.4	12.4	5.8	C	11.1	12.0	6.0
C	11.4	12.4	15.4	C	11.1	12.0	16.1
C	4.4	4.8	5.1	C	4.3	4.6	5.3
C	2.6	2.8	15.4	C	2.5	2.7	16.1
C	9.6	10.4	5.1	C	9.4	10.0	5.3
C	9.6	10.4	16.1	C	9.4	10.0	16.9
C	2.6	2.8	5.8	C	2.5	2.7	6.0
C	11.9	12.9	17.8	C	11.6	12.5	18.7
C	4.9	5.3	7.5	C	4.8	5.1	7.8
C	11.1	12.1	16.7	C	10.9	11.7	17.6
C	4.2	4.5	6.4	C	4.1	4.4	6.7
C	2.1	2.3	17.8	C	2.0	2.2	18.7
C	9.1	9.8	7.5	C	8.9	9.5	7.8
C	2.8	3.0	16.7	C	2.8	2.9	17.6
C	9.8	10.6	6.4	C	9.6	10.3	6.7
C	9.1	9.8	13.6	C	8.9	9.5	14.3
C	2.1	2.3	3.3	C	2.0	2.2	3.5
C	9.8	10.6	14.7	C	9.6	10.3	15.5
C	2.8	3.0	4.4	C	2.8	2.9	4.6
C	4.9	5.3	13.6	C	4.8	5.1	14.3
C	11.9	12.9	3.3	C	11.6	12.5	3.5
C	4.2	4.5	14.7	C	4.1	4.4	15.5

C	11.1	12.1	4.4	C	10.9	11.7	4.6
C	9.8	0.0	20.9	C	9.6	0.0	21.9
C	2.8	7.6	10.6	C	2.8	7.3	11.1
C	8.3	0.0	20.9	C	8.2	0.0	21.9
C	1.4	7.6	10.6	C	1.3	7.3	11.1
C	0.0	10.6	20.9	C	0.0	10.3	21.9
C	7.0	3.1	10.6	C	6.8	3.0	11.1
C	0.0	9.1	20.9	C	0.0	8.8	21.9
C	7.0	1.5	10.6	C	6.8	1.4	11.1
C	4.2	0.0	20.9	C	4.1	0.0	21.9
C	11.1	7.6	10.6	C	10.9	7.3	11.1
C	5.6	0.0	20.9	C	5.5	0.0	21.9
C	12.6	7.6	10.6	C	12.3	7.3	11.1
C	0.0	4.5	20.9	C	0.0	4.4	21.9
C	7.0	12.1	10.6	C	6.8	11.7	11.1
C	0.0	6.1	20.9	C	0.0	5.9	21.9
C	7.0	13.7	10.6	C	6.8	13.2	11.1
C	11.9	2.3	17.8	C	11.6	2.2	18.7
C	4.9	9.8	7.5	C	4.8	9.5	7.8
C	11.1	3.0	16.7	C	10.9	2.9	17.6
C	4.2	10.6	6.4	C	4.1	10.3	6.7
C	4.9	9.8	13.6	C	4.8	9.5	14.3
C	11.9	2.3	3.3	C	11.6	2.2	3.5
C	4.2	10.6	14.7	C	4.1	10.3	15.5
C	11.1	3.0	4.4	C	10.9	2.9	4.6
C	9.1	5.3	13.6	C	8.9	5.1	14.3
C	2.1	12.9	3.3	C	2.0	12.5	3.5
C	9.8	4.5	14.7	C	9.6	4.4	15.5
C	2.8	12.1	4.4	C	2.8	11.7	4.6
C	2.1	12.9	17.8	C	2.0	12.5	18.7
C	9.1	5.3	7.5	C	8.9	5.1	7.8
C	2.8	12.1	16.7	C	2.8	11.7	17.6
C	9.8	4.5	6.4	C	9.6	4.4	6.7
C	9.1	11.4	22.3	C	1.7	0.0	23.3
C	9.8	10.1	22.3	C	1.7	7.3	23.3
C	11.3	10.1	22.3	C	8.5	3.7	23.3
C	12.1	11.4	22.3	C	8.5	11.0	23.3
C	11.3	12.6	22.3	C	6.0	5.0	23.3
C	9.8	12.6	22.3	C	6.0	12.3	23.3
C	11.8	8.8	22.3	C	12.8	1.4	23.3

C	10.6	7.9	22.3	C	12.8	8.7	23.3
C	5.3	12.1	22.3	C	6.0	2.3	23.3
C	5.3	10.7	22.3	C	6.0	9.6	23.3
C	6.8	10.2	22.3	C	12.8	6.0	23.3
C	7.6	11.4	22.3	C	12.8	13.3	23.3
C	4.1	12.8	22.3	C	3.8	6.1	23.3
C	2.8	12.1	22.3	C	3.8	13.4	23.3
C	2.8	10.7	22.3	C	10.6	2.5	23.3
C	4.1	10.0	22.3	C	10.6	9.8	23.3
C	2.9	7.7	22.3	C	6.1	0.0	23.3
C	3.3	6.3	22.3	C	6.1	7.3	23.3
C	4.8	6.3	22.3	C	12.9	3.7	23.3
C	4.1	8.5	22.3	C	12.9	11.0	23.3
C	5.5	5.0	22.3	C	3.8	1.2	23.3
C	4.8	3.8	22.3	C	3.8	8.5	23.3
C	3.3	3.8	22.3	C	10.6	4.9	23.3
C	2.6	5.0	22.3	C	10.6	12.2	23.3
C	9.4	5.6	22.3	H	9.8	10.5	19.0
C	9.8	4.3	22.3	H	3.0	3.2	8.2
C	11.3	4.3	22.3	H	3.9	4.1	19.0
C	10.6	6.5	22.3	H	10.7	11.5	8.2
C	12.1	3.0	22.3	H	10.7	11.5	14.0
C	11.3	1.7	22.3	H	3.9	4.1	3.1
C	9.8	1.7	22.3	H	3.0	3.2	14.0
C	9.1	3.0	22.3	H	9.8	10.5	3.1
C	1.7	0.0	23.7	H	8.1	2.2	21.9
C	1.7	7.6	23.7	H	1.2	9.5	11.1
C	8.7	3.8	23.7	H	2.1	8.6	21.9
C	8.7	11.4	23.7	H	9.0	1.2	11.1
C	6.1	5.2	23.7	H	5.6	12.5	21.9
C	6.1	12.8	23.7	H	12.4	5.1	11.1
C	13.1	1.4	23.7	H	11.5	6.1	21.9
C	13.1	9.0	23.7	H	4.7	13.4	11.1
C	6.1	2.4	23.7	H	11.9	1.9	15.8
C	6.1	10.0	23.7	H	5.1	9.2	4.9
C	13.1	6.2	23.7	H	5.1	9.2	17.2
C	13.1	13.8	23.7	H	11.9	1.9	6.4
C	3.9	6.3	23.7	H	8.6	5.4	17.2
C	3.9	13.9	23.7	H	1.8	12.7	6.4
C	10.9	2.5	23.7	H	1.8	12.7	15.8

C	10.9	10.1	23.7	H	8.6	5.4	4.9
C	6.2	0.0	23.7	H	3.0	11.5	14.0
C	6.2	7.6	23.7	H	9.8	4.1	3.1
C	13.2	3.8	23.7	H	10.7	3.2	14.0
C	13.2	11.4	23.7	H	3.9	10.5	3.1
C	3.9	1.3	23.7	H	3.9	10.5	19.0
C	3.9	8.8	23.7	H	10.7	3.2	8.2
C	10.9	5.0	23.7	H	9.8	4.1	19.0
C	10.9	12.6	23.7	H	3.0	11.5	8.2
H	10.0	10.9	18.2	H	8.1	12.5	21.9
H	3.0	3.3	7.9	H	1.2	5.1	11.1
H	3.9	4.3	18.2	H	2.1	6.1	21.9
H	10.9	11.9	7.9	H	9.0	13.4	11.1
H	10.9	11.9	13.3	H	5.6	2.2	21.9
H	3.9	4.3	3.0	H	12.4	9.5	11.1
H	3.0	3.3	13.3	H	11.5	8.6	21.9
H	10.0	10.9	3.0	H	4.7	1.2	11.1
H	8.2	2.2	20.9	H	5.1	5.4	17.2
H	1.3	9.8	10.6	H	11.9	12.7	6.4
H	2.2	8.8	20.9	H	11.9	12.7	15.8
H	9.2	1.2	10.6	H	5.1	5.4	4.9
H	5.7	12.9	20.9	H	1.8	1.9	15.8
H	12.7	5.3	10.6	H	8.6	9.2	4.9
H	11.8	6.3	20.9	H	8.6	9.2	17.2
H	4.8	13.9	10.6	H	1.8	1.9	6.4
H	12.1	2.0	15.0	H	9.7	8.7	14.3
H	5.1	9.6	4.8	H	2.9	1.4	3.5
H	5.1	9.6	16.4	H	5.6	4.4	14.3
H	12.1	2.0	6.1	H	10.8	13.2	3.5
H	8.8	5.6	16.4	H	6.8	3.0	9.9
H	1.8	13.2	6.1	H	4.1	0.0	20.8
H	1.8	13.2	15.0	H	10.9	7.3	9.9
H	8.8	5.6	4.8	H	1.2	11.7	18.7
H	3.0	11.9	13.3	H	8.0	4.4	7.8
H	10.0	4.3	3.0	H	4.0	8.7	14.3
H	10.9	3.3	13.3	H	10.8	1.4	3.5
H	3.9	10.9	3.0	H	9.7	5.9	14.3
H	3.9	10.9	18.2	H	2.9	13.2	3.5
H	10.9	3.3	7.9	H	12.5	3.0	18.7
H	10.0	4.3	18.2	H	5.6	10.3	7.8

H	3.0	11.9	7.9	H	2.8	7.3	9.9
H	8.2	12.9	20.9	H	0.0	4.4	20.8
H	1.3	5.3	10.6	H	6.8	11.7	9.9
H	2.2	6.3	20.9	H	12.5	11.7	18.7
H	9.2	13.9	10.6	H	4.0	5.9	7.8
H	5.7	2.2	20.9	H	2.9	1.4	18.7
H	12.7	9.8	10.6	H	9.7	8.7	7.8
H	11.8	8.8	20.9	H	1.5	2.2	1.4
H	4.8	1.2	10.6	H	11.7	12.9	1.4
H	5.1	5.6	16.4	H	10.5	1.9	1.7
H	12.1	13.2	6.1	H	3.2	12.8	1.7
H	12.1	13.2	15.0	H	-0.8	1.0	1.5
H	5.1	5.6	4.8	H	-0.8	12.1	1.5
H	1.8	2.0	15.0	H	11.2	-0.8	1.5
H	8.8	9.6	4.8	H	0.9	-0.8	1.5
H	8.8	9.6	16.4	H	9.6	0.0	20.8
H	1.8	2.0	6.1	H	0.0	10.3	20.8
H	9.9	9.1	13.6	H	0.0	10.2	1.4
H	2.9	1.5	3.3	H	9.5	0.0	1.4
H	4.1	6.1	13.6	N	2.4	6.2	23.3
H	11.0	13.7	3.3	N	2.4	13.5	23.3
H	7.0	3.1	9.4	N	9.2	2.5	23.3
H	4.2	0.0	19.7	N	9.2	9.8	23.3
H	11.1	7.6	9.4	N	6.8	6.2	23.3
H	1.2	12.1	17.8	N	6.8	13.5	23.3
H	8.2	4.5	7.5	N	13.6	2.5	23.3
H	4.1	9.1	13.6	N	13.6	9.8	23.3
H	12.7	3.0	3.3	N	4.6	2.4	23.3
H	9.9	6.1	13.6	N	4.6	9.7	23.3
H	2.9	13.7	3.3	N	11.4	6.0	23.3
H	12.7	3.0	17.8	N	11.4	13.4	23.3
H	4.1	9.1	7.5	N	6.8	1.2	23.3
H	2.8	7.6	9.4	N	6.8	8.5	23.3
H	0.0	4.5	19.7	N	13.6	4.9	23.3
H	7.0	12.1	9.4	N	13.6	12.2	23.3
H	11.0	13.7	17.8	N	4.6	5.0	23.3
H	5.7	4.5	7.5	N	4.6	12.3	23.3
H	2.9	1.5	17.8	N	11.4	1.3	23.3
H	9.9	9.1	7.5	N	11.4	8.6	23.3
H	13.1	11.4	22.3	N	2.4	1.2	23.3

H	12.8	8.3	22.3	N	2.4	8.5	23.3
H	8.4	8.3	22.3	N	9.2	4.8	23.3
H	7.0	9.2	22.3	N	9.2	12.2	23.3
H	7.2	13.5	22.3	N	0.0	0.0	23.3
H	4.1	13.9	22.3	N	0.0	7.3	23.3
H	1.8	7.9	22.3	N	6.8	3.7	23.3
H	6.3	7.9	22.3	N	6.8	11.0	23.3
H	6.6	5.0	22.3	N	4.6	0.0	23.3
H	1.5	5.0	22.3	N	4.6	7.3	23.3
H	8.3	5.8	22.3	N	11.4	3.7	23.3
H	12.8	5.8	22.3	N	11.4	11.0	23.3
H	13.1	3.0	22.3	O	2.4	2.5	2.0
H	8.0	3.0	22.3	O	11.3	12.1	2.0
H	9.7	14.6	22.3	O	11.3	2.5	2.0
H	11.5	14.6	22.3	O	2.4	12.1	2.0
H	0.8	10.4	22.3	O	11.3	12.1	20.1
H	1.6	13.7	22.3	O	4.5	4.8	9.3
H	8.1	0.6	22.3	O	2.4	2.5	20.1
H	13.0	0.6	22.3	O	9.2	9.9	9.3
H	1.6	2.7	22.3	O	9.2	9.9	12.9
H	6.5	2.7	22.3	O	4.5	4.8	12.9
H	1.6	2.3	1.3	O	10.2	1.3	21.9
H	11.9	13.3	1.3	O	3.3	8.6	11.1
H	10.7	2.0	1.6	O	1.2	10.9	21.9
H	3.2	13.2	1.6	O	8.1	3.6	11.1
H	-0.8	1.0	1.5	O	3.5	13.3	21.9
H	-0.8	12.5	1.5	O	10.3	6.0	11.1
H	11.5	-0.8	1.5	O	12.4	3.8	21.9
H	0.9	-0.8	1.5	O	5.6	11.1	11.1
H	9.8	0.0	19.7	O	12.5	1.2	18.2
H	0.0	10.6	19.7	O	5.7	8.6	7.3
H	0.0	10.6	1.4	O	5.7	8.6	14.8
H	9.7	0.0	1.4	O	12.5	1.2	4.0
N	9.4	8.8	22.3	O	8.0	6.1	14.8
N	6.8	12.6	22.3	O	1.1	13.4	4.0
N	5.3	7.7	22.3	O	1.1	13.4	18.2
N	11.8	5.6	22.3	O	8.0	6.1	7.3
N	2.4	6.4	23.7	O	4.5	9.9	12.9
N	2.4	13.9	23.7	O	9.2	4.8	12.9
N	9.4	2.6	23.7	O	2.4	12.1	20.1

N	9.4	10.2	23.7	O	9.2	4.8	9.3
N	6.9	6.4	23.7	O	11.3	2.5	20.1
N	6.9	13.9	23.7	O	4.5	9.9	9.3
N	13.9	2.6	23.7	O	10.2	13.3	21.9
N	13.9	10.1	23.7	O	3.3	6.0	11.1
N	4.7	2.4	23.7	O	1.2	3.8	21.9
N	4.7	10.0	23.7	O	8.1	11.1	11.1
N	11.6	6.2	23.7	O	3.5	1.3	21.9
N	11.6	13.8	23.7	O	10.3	8.6	11.1
N	6.9	1.2	23.7	O	12.4	10.9	21.9
N	6.9	8.8	23.7	O	5.6	3.6	11.1
N	13.9	5.0	23.7	O	5.7	6.1	14.8
N	13.9	12.6	23.7	O	12.5	13.4	4.0
N	4.7	5.1	23.7	O	12.5	13.4	18.2
N	4.7	12.7	23.7	O	5.7	6.1	7.3
N	11.6	1.4	23.7	O	1.1	1.2	18.2
N	11.6	8.9	23.7	O	8.0	8.6	7.3
N	2.4	1.2	23.7	O	8.0	8.6	14.8
N	2.4	8.8	23.7	O	1.1	1.2	4.0
N	9.4	5.0	23.7	O	0.0	1.8	1.5
N	9.4	12.6	23.7	O	0.0	12.9	1.5
N	0.0	0.0	23.7	O	12.0	0.0	1.5
N	0.0	7.6	23.7	O	1.6	0.0	1.5
N	7.0	3.8	23.7	O	12.0	0.0	20.6
N	7.0	11.4	23.7	O	5.2	7.3	9.8
N	4.7	0.0	23.7	O	1.6	0.0	20.6
N	4.7	7.6	23.7	O	8.5	7.3	9.8
N	11.6	3.8	23.7	O	6.8	9.1	12.4
N	11.6	11.4	23.7	O	6.8	5.6	12.4
O	2.4	2.6	2.0	O	5.2	7.3	12.4
O	11.5	12.5	2.0	O	8.5	7.3	12.4
O	11.5	2.6	2.0	O	0.0	12.9	20.6
O	2.4	12.5	2.0	O	6.8	5.6	9.8
O	9.1	13.9	22.3	O	0.0	1.8	20.6
O	12.1	13.9	22.3	O	6.8	9.1	9.8
O	1.5	10.0	22.3	Zr	12.1	13.0	21.9
O	1.5	12.8	22.3	Zr	5.3	5.7	11.1
O	9.1	0.5	22.3	Zr	1.5	1.6	21.9
O	12.1	0.5	22.3	Zr	8.4	9.0	11.1
O	2.6	2.5	22.3	Zr	12.1	1.6	21.9

O	5.5	2.5	22.3	Zr	5.3	9.0	11.1
O	11.5	12.5	19.1	Zr	1.5	13.0	21.9
O	4.6	5.0	8.8	Zr	8.4	5.7	11.1
O	2.4	2.6	19.1	Zr	0.0	0.0	19.5
O	9.4	10.2	8.8	Zr	6.8	7.3	8.6
O	9.4	10.2	12.3	Zr	6.8	7.3	13.5
O	4.6	5.0	12.3	Zr	0.0	0.0	2.6
O	10.4	1.4	20.9				
O	3.4	8.9	10.6				
O	1.2	11.3	20.9				
O	8.2	3.7	10.6				
O	3.6	13.8	20.9				
O	10.6	6.2	10.6				
O	12.7	3.9	20.9				
O	5.7	11.5	10.6				
O	12.8	1.3	17.3				
O	5.8	8.8	7.0				
O	5.8	8.8	14.1				
O	12.8	1.3	3.8				
O	8.1	6.3	14.1				
O	1.2	13.9	3.8				
O	1.2	13.9	17.3				
O	8.1	6.3	7.0				
O	4.6	10.2	12.3				
O	9.4	5.0	12.3				
O	2.4	12.5	19.1				
O	9.4	5.0	8.8				
O	11.5	2.6	19.1				
O	4.6	10.2	8.8				
O	10.4	13.8	20.9				
O	3.4	6.2	10.6				
O	1.2	3.9	20.9				
O	8.2	11.5	10.6				
O	3.6	1.4	20.9				
O	10.6	8.9	10.6				
O	12.7	11.3	20.9				
O	5.7	3.7	10.6				
O	5.8	6.3	14.1				
O	12.8	13.9	3.8				
O	12.8	13.9	17.3				

O	5.8	6.3	7.0
O	1.2	1.3	17.3
O	8.1	8.8	7.0
O	8.1	8.8	14.1
O	1.2	1.3	3.8
O	0.0	1.8	1.5
O	0.0	13.3	1.5
O	12.3	0.0	1.5
O	1.7	0.0	1.5
O	12.3	0.0	19.6
O	5.3	7.6	9.3
O	1.7	0.0	19.6
O	8.7	7.6	9.3
O	7.0	9.4	11.8
O	7.0	5.8	11.8
O	5.3	7.6	11.8
O	8.7	7.6	11.8
O	0.0	13.3	19.6
O	7.0	5.8	9.3
O	0.0	1.8	19.6
O	7.0	9.4	9.3
Zr	12.4	13.5	20.9
Zr	5.4	5.9	10.6
Zr	1.6	1.7	20.9
Zr	8.5	9.3	10.6
Zr	12.4	1.7	20.9
Zr	5.4	9.3	10.6
Zr	1.6	13.5	20.9
Zr	8.5	5.9	10.6
Zr	0.0	0.0	18.5
Zr	7.0	7.6	8.3
Zr	7.0	7.6	12.9
Zr	0.0	0.0	2.6

Table S5 Photocatalytic NH_3 evolution rate of UiO-66, CNNS, UC and UPC photocatalysts.

Photocatalysts	**Light source**	
	Full spectrum	**Visible light（λ ≥ 420 nm）**
UiO-66	78.14 μmol h^{-1} g^{-1}	10.34 μmol h^{-1} g^{-1}

CNNS	41.52 μmol h^{-1} g^{-1}	19.83 μmol h^{-1} g^{-1}
UC	85.60 μmol h^{-1} g^{-1}	14.24 μmol h^{-1} g^{-1}
UPC	147.76 μmol h^{-1} g^{-1}	62.41 μmol h^{-1} g^{-1}

Table S6 Photocatalytic NH_3 evolution rate of photocatalysts.

Photocatalysts	**Light source**	**Detection method**	**NH_3 evolution rate ($\mu mol\ h^{-1}\ g^{-1}$)**	**Reference**
MIL-101(Fe)	Full spectrum	NR [a]	50.4	[14]
ZIF-67@PMo_4V_8	Full spectrum	NR [a]	149.0	[15]
Ti_3C_2-QD/Ni-MOF	Full spectrum	NR [a]	88.8	[16]
Al-PMOF(Fe)	≥420 nm	IB [b]	7.1	[17]
MOF-76(Ce)	Full spectrum	IB [b]	34.0	[18]
Cu-TiO_2	200-800 nm	IC [c]	78.9	[19]
MoO_{3-x}	≥300 nm	IC [c]	11.1	[20]
NH_2-MIL-125 (Ti)	≥400 nm	IC [c]	12.3	[21]
Cu_2O	≥400 nm	IC [c]	30.3	[22]
U(0.5Hf)-2SH	≥420 nm	IC [c]	116.1	[5]
g-C_3N_4	≥420 nm	IC [c]	105.0	[23]
UPC	≥420 nm	IC [c]	62.4	This work
NU6(Ce-Hf)	Full spectrum	IC [c]	158.4	[24]
UPC	Full spectrum	IC [c]	147.8	This work

[a] The detection method of Nessler's reagent.

[b] The detection method of indophenol blue.

[c] The detection method of ion chromatography.

Table S7 The absorption edge, band gap (E_g), conduction band potential (E_{cb}) and valence band potential (E_{vb}) of UiO-66 and CNNS samples.

Photocatalysts	Absorption edges (nm)	E_g (eV)	E_{cb} (V)	E_{vb} (V)
UiO-66	308	4.01	-0.55	3.46
CNNS	427	2.91	-0.92	1.99

Table S8 Calculated AQE of UPC at different wavelengths.

Wavelength λ (nm)	Light power density I (mW cm^{-2})	Light power P (mW)	NH_3 evolution rate (μmol h^{-1} g^{-1})	AQE (%)
380	65	2156	70.20	0.86%
405	54	1791	56.56	0.78%
420	60	1990	62.41	0.75%
450	72	2388	75.17	0.70%
500	66	2189	74.70	0.68%

Taking the $\lambda = 380\ \mathrm{nm}$ as an example, the AQE was calculated according to the following equation:

The diameter of the reactor is 6.5 cm. The irradiation area of the solution is:

$$S = \pi \times (\frac{d}{2})^2 = 3.14 \times 3.25^2 = 33.17\ \mathrm{cm}^2$$

The light power is

$$P = I \times S = 65 \times 33.17 = 2156\ \mathrm{mW}$$

The number of the incident photons at 380 nm is

$$N_{incident} = \frac{Pt}{h\upsilon} = \frac{Pt\lambda}{hc} = \frac{2156 \times 10^{-3} \times 3600 \times 380 \times 10^{-9}}{6.63 \times 10^{-34} \times 3 \times 10^{8}} = 1.48 \times 10^{22}$$

The number of reacted electrons is

$$N_{reacted} = 3 \times N_{(NH_3)} = 3 \times n_{(NH_3)} \times N_A = 3 \times 70.20 \times 10^{-6} \times 6.02 \times 10^{23} = 1.27 \times 10^{20}$$

The AQE can be calculated as

$$AQE = \frac{N_{reacted}}{N_{incident}} \times 100\% = \frac{1.27 \times 10^{20}}{1.48 \times 10^{22}} \times 100\% = 0.86\%$$

The STA efficiency was calculated according to the following equation:

The light power is

$$P = I \times S = 304 \times 33.17 = 10084\ mW$$

The STA efficiency can be calculated as

$$\text{STA efficiency} = \frac{\Delta G_{(NH_3)} \times n_{(NH_3)}}{Pt} \times 100\% = \frac{339 \times 10^3 \times 147.8 \times 10^{-6}}{10084 \times 10^{-3} \times 3600} \times 100\% = 0.14\%$$

6. References

[1] Zhao, Y.; Truhlar, D. G. Density functionals with broad applicability in chemistry. *Acc. Chem. Res.* **2008**, *41* (2), 157-167.

[2] Grimme, S.; Antony, J.; Ehrlich, S.; Krieg, H. A consistent and accurate ab initio parametrization of density functional dispersion correction (DFT-D) for the 94 elements H-Pu. *J. Chem. Phys.* **2010**, *132* (15), 154104.

[3] Segall, M. D.; Lindan, P. J. D.; Probert, M. J.; Pickard, C. J.; Hasnip, P. J.; Clark, S. J.; Payne, M. C. First-principles simulation: ideas, illustrations and the CASTEP code. *J. Phys.: Condens. Matter.* **2002**, 14 (11), 2717-2744.

[4] Clark, S. J.; Segall, M. D.; Pickard, C. J.; Hasnip, P. J.; Probert, M. J.; Refson, K.; Payne, MC. First principles methods using CASTEP. *Zeits. für Kris.-Crystal. Mater.* **2005**, *220* (5-6), 567-570.

[5] An, K.; Ren, H. J.; Yang, D.; Zhao, Z. F.; Gao, Y. C.; Chen, Y.; Tan, J. D.; Wang, W. J.; Jiang, Z. Y. Nitrogenase-inspired bimetallic metal organic frameworks for visible-light-driven nitrogen fixation. *Appl. Catal. B-Environ.* **2021**, *292*, 120167.

[6] Oien, S.; Wragg, D.; Reinsch, H.; Svelle, S.; Bordiga, S.; Lamberti, C.; Lillerud, K. P. Detailed structure analysis of atomic positions and defects in zirconium metal-organic frameworks. *Cryst. Growth Des.* **2014**, *14* (11), 5370-5372.

[7] Banerjee, D.; Xu, W. Q.; Nie, Z. M.; Johnson, L. E. V.; Coghlan, C.; Sushko, M. L.; Kim, D.; Schweiger, M. J.; Kruger, A. A.; Doonan, C. J.; Thallapally, P. K. Zirconium-based metal-organic framework for removal of perrhenate from water. *Inorg. Chem.* **2016**, *55* (17), 8241-8243.

[8] Ren, H. J.; Yang, D.; Ding, F.; An, K.; Zhao, Z. F.; Chen, Y.; Zhou, Z. Y.; Wang, W.

J.; Jiang, Z. Y. One-pot fabrication of porous nitrogen-deficient g-C_3N_4 with superior photocatalytic performance. *J. Photochem. Photobiol. A-Chem.* **2020**, *400*, 112729.

[9] Basharnavaz, H.; Habibi-Yangjeh, A.; Mousavi, M. Ni, Pd, and Pt-embedded graphitic carbon nitrides as excellent adsorbents for HCN removal: a DFT study. *Appl. Surf. Sci.* **2018**, *456*, 882-889.

[10] Niu, P.; Liu, G.; Cheng, H. M. Nitrogen vacancy-promoted photocatalytic activity of graphitic carbon nitride. *J. Phys. Chem. C* **2012**, *116* (20), 11013-11018.

[11] Wu, Z. G.; Cohen, R. E. More accurate generalized gradient approximation for solids. *Phys. Rev. B* **2006**, 73 (23), 235116.

[12] Perdew, J. P.; Ruzsinszky, A.; Csonka, G. I.; Vydrov, O. A.; Scuseria, G. E.; Constantin, L. A.; Zhou, X. L.; Burke, K. Restoring the density-gradient expansion for exchange in solids and surfaces. *Phys. Rev. Lett.* **2008**, *100* (13), 136406.

[13] Akkermans, R. L. C.; Spenley, N. A.; Robertson, S. H. Monte Carlo methods in Materials Studio. *Mol. Simul.* **2013**, *39* (14-15), 1153-1164.

[14] Li, G. Q.; Li, F. F.; Liu, J. X.; Fan, C. M. Fe-based MOFs for photocatalytic N_2 reduction: Key role of transition metal iron in nitrogen activation. *J. Solid State Chem.* **2020**, *285*, 121245.

[15] Li, X. H.; He, P.; Wang, T.; Zhang, X. W.; Chen, W. L.; Li, Y. G. Keggin-type polyoxometalate-based ZIF-67 for enhanced photocatalytic nitrogen fixation. *ChemSusChem* **2020**, *13* (10), 2769-2778.

[16] Qin, J. Z.; Liu, B. J.; Lam, K. H.; Song, S. J.; Li, X. Y.; Hu, X. 0D/2D MXene quantum dot/Ni-MOF ultrathin nanosheets for enhanced N_2 photoreduction. *ACS Sustainable Chem. Eng*. **2020**, *8* (48), 17791-17799.

[17] Shang, S. S.; Xiong, W.; Yang, C.; Johannessen, B.; Liu, R. G.; Hsu, H. Y.; Gu, Q. F.; Leung, M. K. H.; Shang, J. Atomically dispersed iron metal site in a porphyrin-based metal-organic framework for photocatalytic nitrogen fixation. *ACS Nano* **2021**, *15* (6), 9670-9678.

[18] Zhang, C. M.; Xu, Y. L.; Lv, C. D.; Zhou, X.; Wang, Y.; Xing, W. N.; Meng, Q. Q.;

Kong, Y.; Chen, G. Mimicking π backdonation in Ce-MOFs for solar-driven ammonia synthesis. *ACS Appl. Mater. Interfaces* **2019**, *11* (33), 29917-29923.

[19] Zhao, Y. X.; Zhao, Y. F.; Shi, R.; Wang, B.; Waterhouse, G. I. N.; Wu, L. Z.; Tung, C. H.; Zhang, T. R. Tuning oxygen vacancies in ultrathin TiO_2 nanosheets to boost photocatalytic nitrogen fixation up to 700 nm. *Adv. Mater.* **2019**, *31* (16), 1806482.

[20] Li, Y. H.; Chen, X.; Zhang, M. J.; Zhu, Y. M.; Ren, W. J.; Mei, Z. W.; Gu, M.; Pan, F. Oxygen vacancy-rich MoO_{3-x} nanobelts for photocatalytic N_2 reduction to NH_3 in pure water. *Catal. Sci. Technol.* **2019**, *9* (3), 803-810.

[21] Huang, H.; Wang, X. S.; Philo, D.; Ichihara, F.; Song, H.; Li, Y. X.; Li, D.; Qiu, T.; Wang, S. Y.; Ye, J. H. Toward visible-light-assisted photocatalytic nitrogen fixation: A titanium metal organic framework with functionalized ligands. *Appl. Catal. B-Environ.* **2020**, *267*, 118686.

[22] Zhang, S.; Zhao, Y. X.; Shi, R.; Zhou, C.; Waterhouse, G. I. N.; Wang, Z.; Weng, Y. X.; Zhang, T. R. Sub-3 nm ultrafine Cu_2O for visible light driven nitrogen fixation. *Angew. Chem. Int. Ed.* **2021**, *60* (5), 2554-2560.

[23] Qi, Y. F.; Chen, Y. F.; Wang, R.; Wang, L. J.; Zhang, F. L.; Shen, Q.; Qu, P.; Liu, D. S. Zinc-deficiency induced g-C_3N_4 nanosheets: photocatalytic nitrogen fixation study and carrier dynamics. *Catal. Lett.* **2020**, *151* (6), 1546-1555.

[24] An, K.; Tan, J. D.; Yang, D.; Ren, H. J.; Zhao, Z. F.; Chen, Y.; Wang, W. J.; Xin, X.; Shi, Y. H.; Jiang, Z. Y. Modular assembly of electron transfer pathways in bimetallic MOFs for photocatalytic ammonia synthesis. *Catal. Sci. Technol.* **2022**, *12* (6), 2015-2022.